

Basic Transverse H-Field Formulation

$$\frac{\partial^2 \mathbf{H}}{\partial x^2} + \frac{\partial^2 \mathbf{H}}{\partial y^2} + \frac{\partial^2 \mathbf{H}}{\partial z^2} + k_0^2 n^2 \mathbf{H} = 0 \quad (1)$$

$$\frac{d^2 \bar{\mathbf{H}}}{dz^2} + \bar{Q}^2 \bar{\mathbf{H}} = \bar{\mathbf{0}} \quad (2)$$

$$\bar{\mathbf{H}} \equiv \begin{pmatrix} \bar{H}_x & \bar{H}_y \end{pmatrix}^T$$

$$\bar{\mathbf{H}} = e^{j\bar{Q}z} \bar{\mathbf{A}} + e^{-j\bar{Q}z} \bar{\mathbf{B}} \quad (3)$$

$$\bar{\mathbf{E}} = \bar{\mathbf{S}} \bar{\mathbf{H}} \quad (4)$$

$$\bar{\mathbf{E}} \equiv \begin{pmatrix} \bar{E}_y & -\bar{E}_x \end{pmatrix}^T$$

$$\bar{\mathbf{S}} = \left(j \sqrt{\mu_0 / \varepsilon_0} / k_0 \right) \bar{N}^{-2} \left(\bar{\mathbf{O}} - \bar{Q}^2 \right) \left(j \bar{Q} \right)^{-1} \quad (5)$$

Application to Multiple Longitudinal Discontinuities

$$\bar{H}_m = e^{j\bar{Q}_m(z-z_{m-1})}\bar{A}_m + e^{-j\bar{Q}_m(z-z_m)}\bar{B}_m \quad (6)$$

$$\bar{P}_m \bar{A}_m + \bar{B}_m = \bar{A}_{m+1} + \bar{P}_{m+1} \bar{B}_{m+1} \quad (7 \text{ a})$$

$$\bar{S}_m (\bar{P}_m \bar{A}_m - \bar{B}_m) = \bar{S}_{m+1} (\bar{A}_{m+1} - \bar{P}_{m+1} \bar{B}_{m+1}) \quad (7 \text{ b})$$

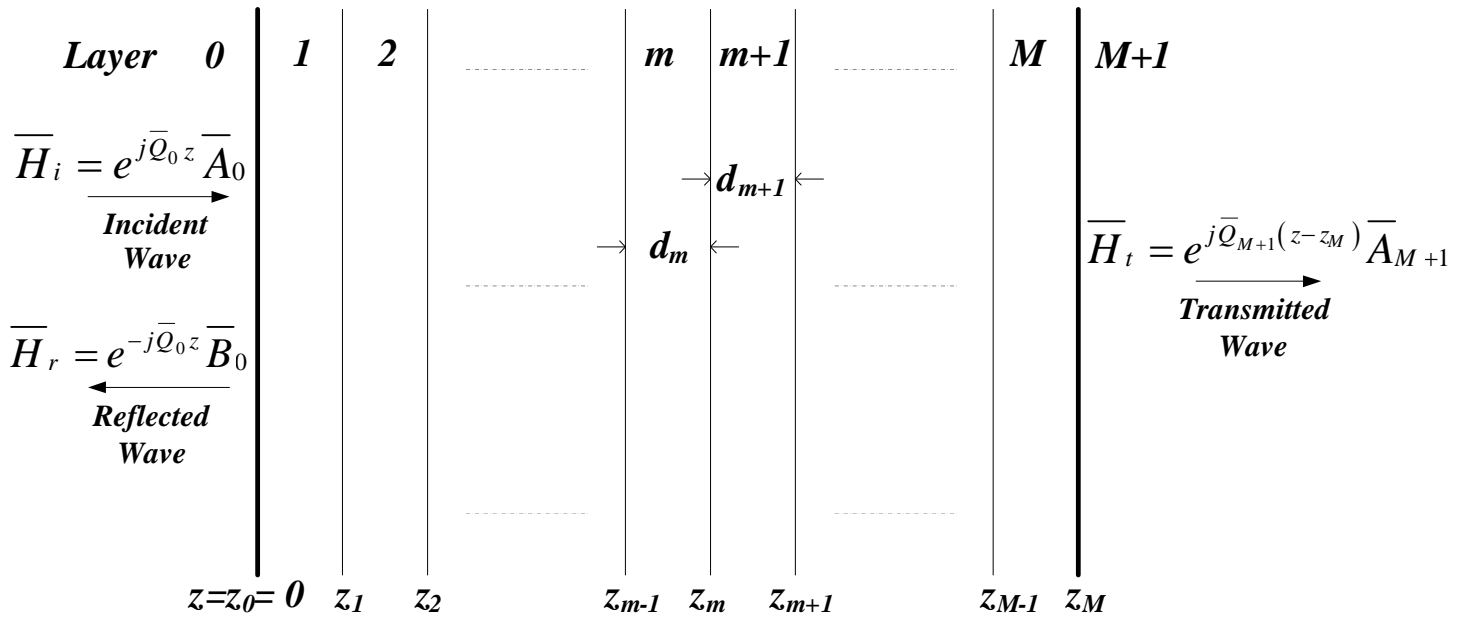


Figure 1: Multi-layer structure with abrupt longitudinal discontinuities. The incident and reflected fields exist within the left most layer and the transmitted field exists within the right most layer.

$$\bar{\Gamma}\bar{X} = \begin{bmatrix} \bar{\Gamma}_{11} & \bar{\Gamma}_{12} \\ \bar{\Gamma}_{21} & \bar{\Gamma}_{22} \end{bmatrix} \begin{bmatrix} \bar{X}_1 \\ \bar{X}_2 \end{bmatrix} = \begin{bmatrix} \bar{\Lambda}_1 \\ \bar{\Lambda}_2 \end{bmatrix} = \bar{\Lambda} \quad (8)$$

Where

$$\bar{\Gamma}_{11} = \begin{bmatrix} \bar{U}_0 & \bar{Y}_1 & & & & \\ & \bar{U}_1 & \bar{Y}_2 & & & \\ & & \ddots & \ddots & & \\ & & & \ddots & \ddots & \\ & & & & \ddots & \bar{Y}_M \\ & & & & & \bar{U}_M \end{bmatrix}$$

$$\bar{\Gamma}_{12} = \begin{bmatrix} \bar{0} & & & & & \\ \bar{V}_1 & \ddots & & & & \\ & \bar{V}_2 & \ddots & & & \\ & & \ddots & \ddots & & \\ & & & \ddots & \ddots & \\ & & & & \bar{V}_M & \bar{0} \end{bmatrix}$$

$$\bar{\Gamma}_{21} = \begin{bmatrix} \bar{0} & \bar{Z}_1 & & & & \\ & \ddots & \bar{Z}_2 & & & \\ & & \ddots & \ddots & & \\ & & & \ddots & \ddots & \\ & & & & \ddots & \bar{Z}_M \\ & & & & & \bar{0} \end{bmatrix}$$

$$\bar{\Gamma}_{22} = \begin{bmatrix} \bar{U}_0 & & & & & \\ \bar{Y}_1 & \bar{U}_1 & & & & \\ & \bar{Y}_2 & \ddots & & & \\ & & \ddots & \ddots & & \\ & & & \ddots & \ddots & \\ & & & & \bar{Y}_M & \bar{U}_M \end{bmatrix}$$

$$\bar{X}_1 = [\bar{B}_0 \quad \bar{B}_1 \quad \cdots \quad \bar{B}_{M-1} \quad \bar{B}_M]^T$$

$$\bar{X}_2 = [\bar{A}_1 \quad \bar{A}_2 \quad \cdots \quad \bar{A}_M \quad \bar{A}_{M+1}]^T$$

$$\bar{\Lambda}_1 = [(\bar{S}_0 - \bar{S}_1)\bar{A}_0 \quad \bar{0} \quad \cdots \quad \bar{0} \quad \bar{0}]^T$$

$$\bar{\Lambda}_2 = [(2\bar{S}_0\bar{A}_0) \quad \bar{0} \quad \cdots \quad \bar{0} \quad \bar{0}]^T$$

$$\bar{U}_m = \bar{S}_m + \bar{S}_{m+1}$$

$$\bar{Y}_m = -2\bar{S}_m\bar{P}_m$$

$$\bar{V}_m = -(\bar{S}_m - \bar{S}_{m+1})\bar{P}_m$$

$$\bar{Z}_m = (\bar{S}_{m-1} - \bar{S}_m)\bar{P}_m$$

Full Padé Approach

$$\bar{Q} = \alpha^{-1/2} \sqrt{\bar{I} + \bar{F}} = \alpha^{-1/2} \prod_{k=1}^4 \frac{\bar{I} + a_k^{(4)} \bar{F}}{\bar{I} + b_k^{(4)} \bar{F}} \quad (9)$$

$$\bar{P} = e^{j\bar{Q}d} = e^{j\alpha^{-1/2} \sqrt{\bar{I} + \bar{F}} d} = \prod_{k=1}^8 c_k^{(8)} \frac{\bar{I} + d_k^{(8)} \bar{F}}{\bar{I} + e_k^{(8)} \bar{F}} \quad (10)$$

$$\bar{F} \equiv \alpha \bar{Q}^2 - \bar{I}$$

Hybrid Approach

$$\bar{P} = e^{j\bar{Q}d} \approx \bar{T} e^{j\bar{C}d} \bar{G} \quad (11)$$

$\bar{T} = \bar{T}_{2pq \times r}$ is the eigenvector matrix with r eigenvectors of \bar{Q}^2

$\bar{C} = \bar{C}_{r \times r}$ = diagonal matrix which contains r eigenvalues

$\bar{G} = \bar{G}_{r \times 2pq}$ = the pseudo-inverse of \bar{T}

Numerical Results

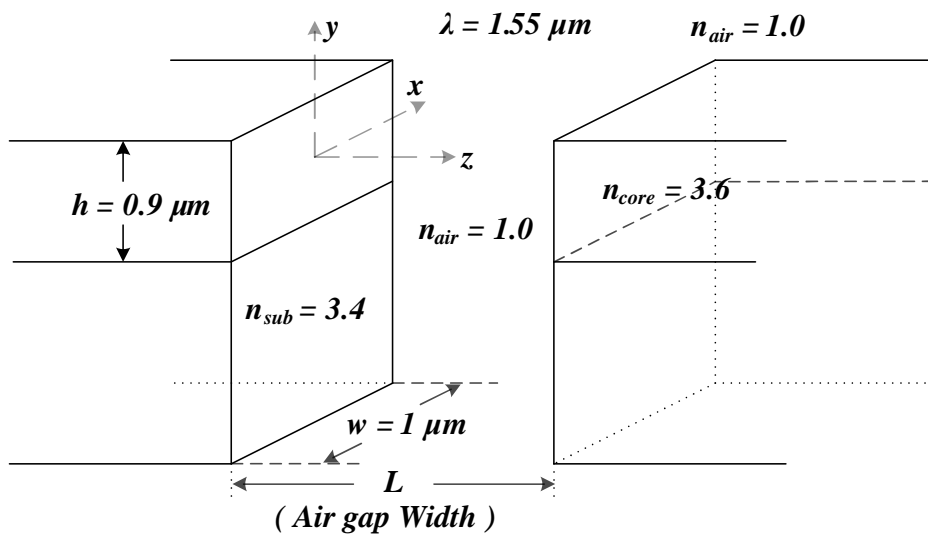


Figure 2: Two identical channel waveguides with an air gap.

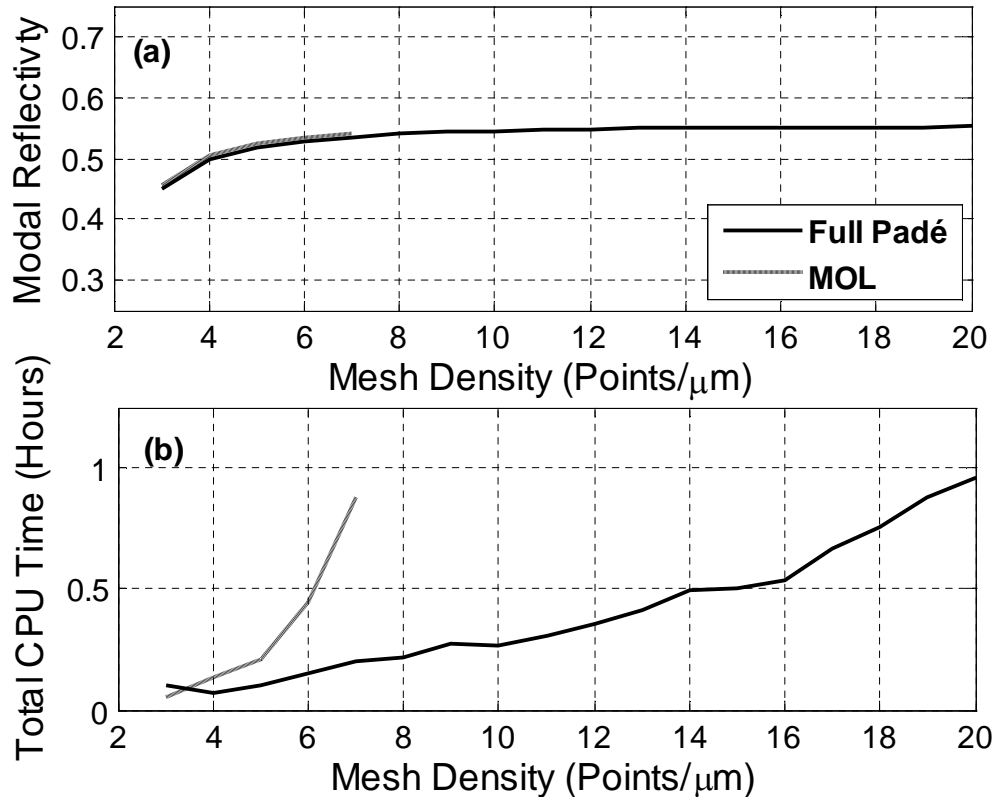


Figure 3: (a) Variation of the fundamental $TE - Like$ modal reflectivity as a function of transverse mesh density. The results correspond to the structure depicted in Figure 2 for a fixed air gap width of $0.5\mu m$. The results of the full Padé approach and the MOL numerical technique are shown. (b) The CPU runtime requirement corresponding to Figure 3 (a).

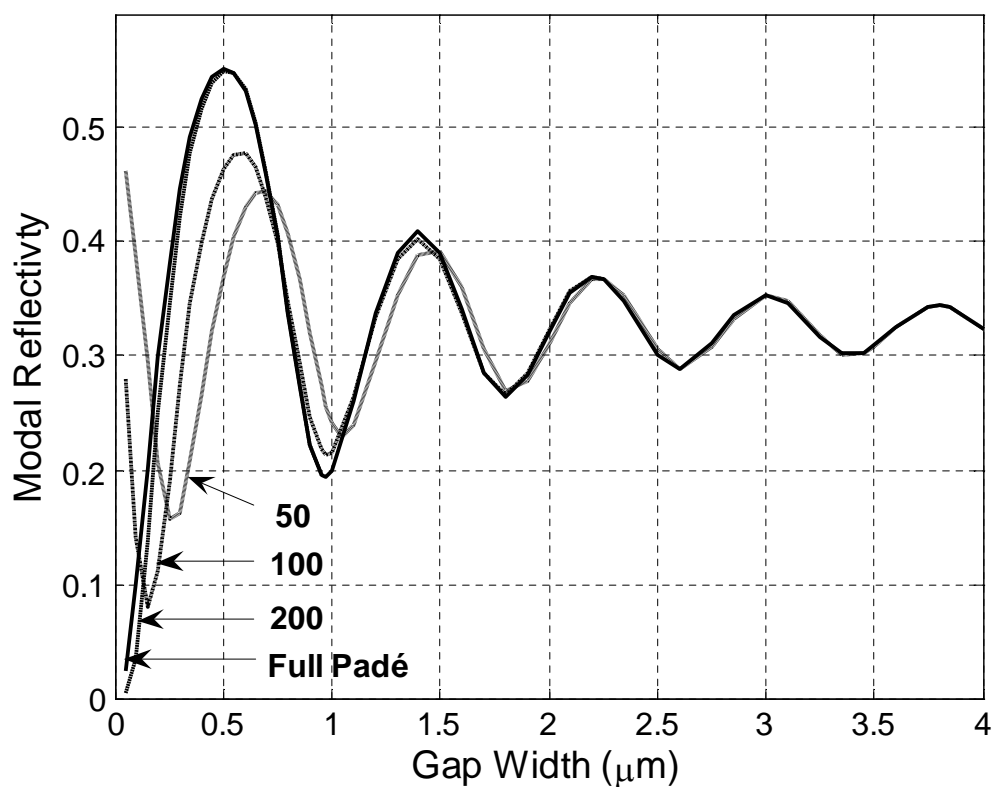


Figure 4: Variation of the fundamental *TE - Like* modal reflectivity as a function of air gap width. The results correspond to the structure depicted in Figure 2. The results of the full Padé and of the hybrid approach using 50, 100, and 200 eigenpairs are shown.

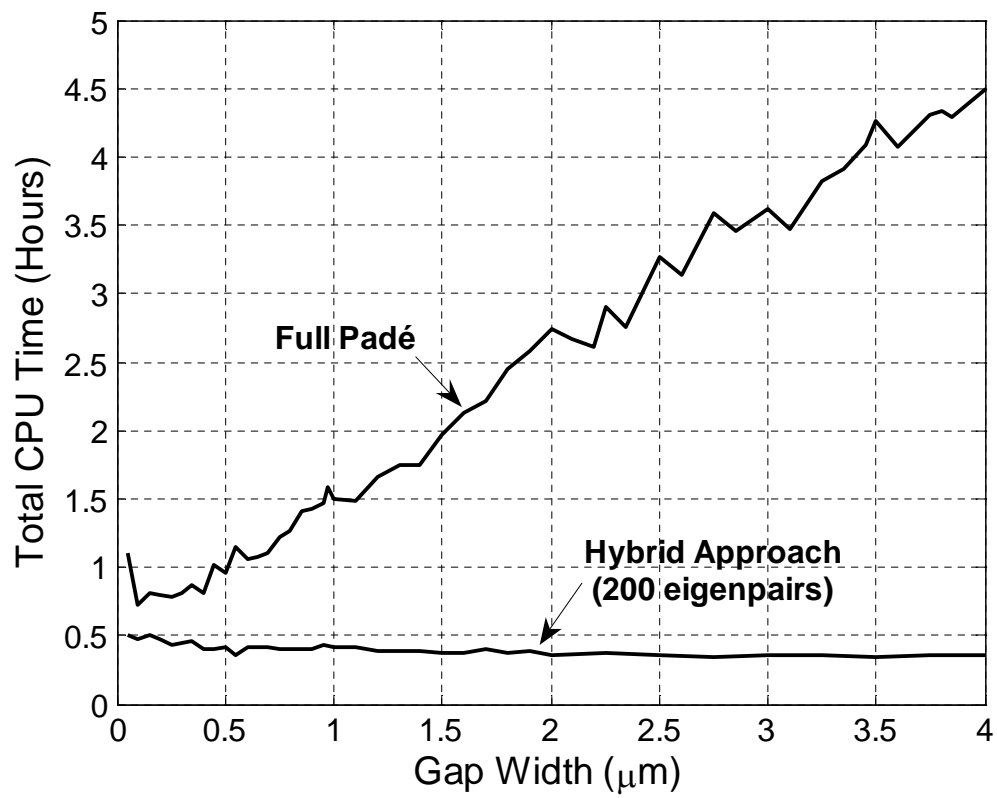


Figure 5: CPU time requirement corresponding to Figure 4.

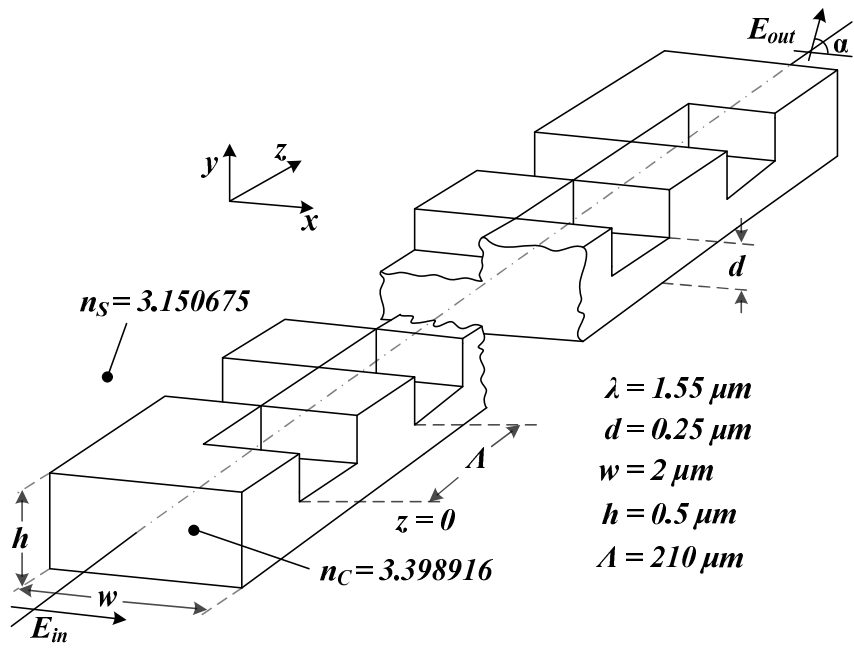


Figure 6: Guided wave polarization rotator.

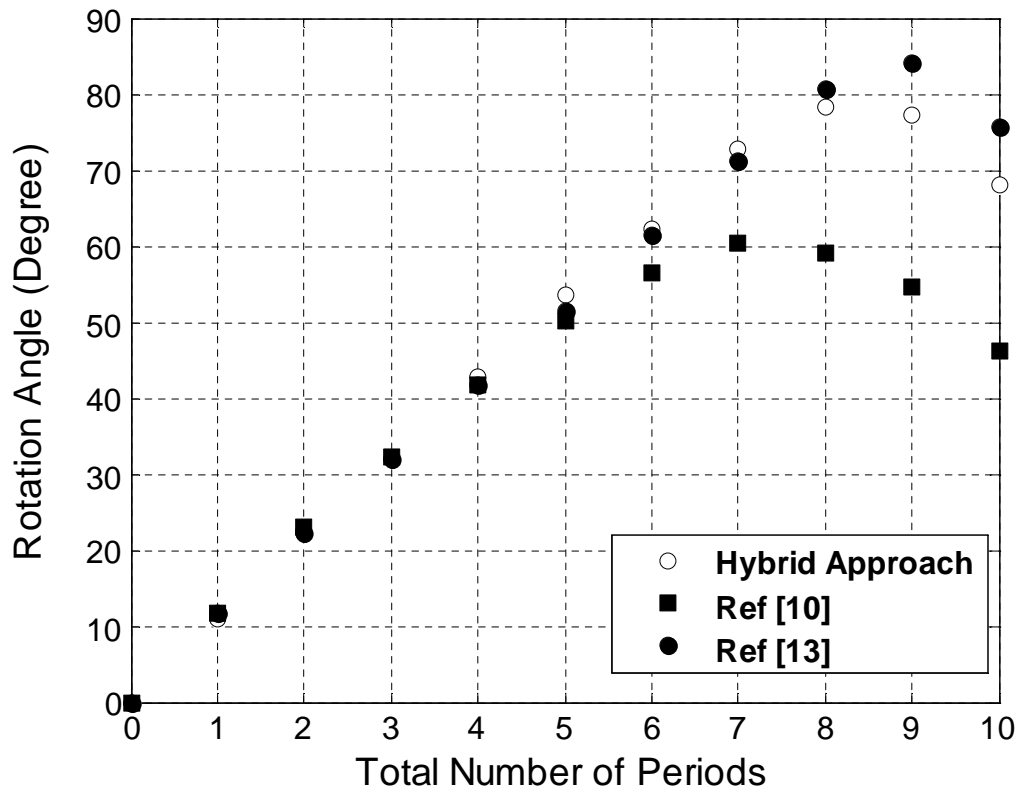


Figure 7: Rotation angle and as a function of the total number of periods. The curves show the results of the hybrid approach and previously reported results.